

**Title: Large Impact of obesity on the disposition of ivermectin, moxidectin and eprinomectin in a canine model: relevance for COVID-19 patients.**

**Short running title:** obesity and pharmacokinetics of ivermectin, moxidectin and eprinomectin

**Authors:**

A. Bousquet-Mélou<sup>1</sup>, A Lespine<sup>1</sup>, J-F Sutra<sup>1</sup>, I Bargues<sup>1</sup>, P-L. Toutain<sup>1,3</sup>

<sup>1</sup> *INTHERES, Université de Toulouse, INRAE, ENVT, Toulouse, France.*

<sup>3</sup> *The Royal Veterinary College, Hawkshead Campus, Hatfield, Herts., AL9 7TA, United Kingdom*

**Orcid numbers**

Bousquet-Melou: <https://orcid.org/0000-0002-7661-4311>

P-L Toutain: <http://orcid.org/0000-0002-8846-8892>

\*Corresponding author: *Pierre-Louis Toutain\**

E-mail to : [pltoutain@wanadoo.fr](mailto:pltoutain@wanadoo.fr) Fax: +33 561 19 39 17

**Word count: 3880**

**Bullet point summary:**

**‘What is already known’,**

- The parasiticide Ivermectin is currently being evaluated for the prevention and treatment of COVID-19, a condition for which obesity is a major risk factor.
- Dosages of ivermectin and moxidectin, an analog of ivermectin, are based on total body weight and there are no recommendations to adjust dosage in obese patients.

### **'What this study adds'**

- Using a canine model of obesity, it was shown that the absolute value (expressed in L/day) of plasma clearance is unchanged for moxidectin and reduced for ivermectin in obesity compared to control conditions, whilst steady-state volumes of distribution (expressed in L) were increased.

### **'Clinical significance',**

- It is suggested that maintenance doses of ivermectin and moxidectin that are controlled by clearance must be based on lean body weight (individual flat dose) while the loading doses that are controlled by the volume of distribution should be based on actual total body weight.

### **Abstract:**

#### **Background and Purpose:**

Based on *in vitro* data, ivermectin (IVM) has been proposed for the prevention and treatment of COVID-19, a condition for which obesity is a major risk factor. IVM dosage is based on total body weight and there are no recommendations to adjust dosage in obese patients. The objective of this study was to establish, in a canine model, the influence of obesity on the clearance and steady-state volume of distribution of IVM and two analog compounds, moxidectin (MOX) and eprinomectin (EPR).

#### **Experimental Approach:**

An experimental model of obesity in dogs was based on a high calorie diet. IVM, MOX and EPR were administered intravenously, simultaneously in combination, to a single group of dogs in two circumstances, during a control period and when body weight had been increased by 50%.

#### **Key Results:**

In obese dogs, clearance, expressed in absolute values (L/day), was not modified for MOX and reduced for IVM and EPR, compared to the initial control state. When scaled by body weight (L/day/kg), plasma clearance was reduced by 42, 55 and

63%, for MOX, IVM and EPR, respectively. In contrast, the steady-state volume of distribution was markedly increased in absolute values (L) by obesity.

### **Conclusion and Implications:**

For IVM and MOX, the obese dog model suggests that the maintenance dose should not be adjusted by total body weight in the obese subject but should be based on lean body weight. On the other hand, the loading dose should be computed based on the total body weight of the obese subject.

### **Abbreviations**

**CL:** Clearance

**Cl<sub>d</sub>:** Clearance of distribution

**EPR:** Eprinomectin

**IVM :** Ivermectin

**LBW:** Lean Body Weight

**MOX:** Moxidectin

**MRT:** Mean Residence Time

**Total Body Weight:** TBW

**V<sub>c</sub>:** Volume of the central compartment

**V<sub>2</sub> & V<sub>3</sub>:** Volume of compartment 2 & 3 respectively

**V<sub>area</sub> or V<sub>z</sub>:** Volume of distribution associated to the terminal phase

**VPC:** Visual Predictive Check

**V<sub>ss</sub>:** Steady-State volume of distribution

**Key words:** ivermectin, moxidectin, obesity, dosage regimen, canine model, pharmacokinetics, COVID-19.

### **Introduction:**

Ivermectin (IVM) is a broad spectrum macrocyclic antiparasitic drug, active against internal parasites (nematodes) and ectoparasites (arthropods) (Fox, 2006). It is used in both human and veterinary medicine. It has been recommended for extensive use in humans for prevention of onchocerciasis (*Onchocerca volvulus*) and to combat river blindness (Cupp et al., 2011). Recent *in vitro* studies, using Vero-hSLAM cells, demonstrated that IVM has a virucidal action against coronavirus-2 (SARS-Cov-2) (Caly et al., 2020) as well as several other viruses (Heidary & Gharebaghi, 2020). These data raised the expectation that IVM might be used in combination with other drugs for the treatment of COVID-19. It is currently undergoing assessment in clinical interventional treatment in 45 clinical trials (Anonymous, 2020a) involving IVM listed in the data base Clinical trial.gov of the U.S. National Library of Medicine. However, virucidal concentrations *in vitro* (5000 nmol/L) were much higher, by several orders of magnitude, than those required for an antiparasitic effects achieved *in vivo*. This led several authors to cast doubts on the potential benefits of systemic IVM administration for prevention of COVID-19 or use in its treatment (Bray et al., 2020). Despite these reservations, IVM is widely used off-label to prevent or to treat COVID-19 and even approved in certain countries (Vora et al., 2020).

The oral dosage of IVM is body-weight-based with a typical recommended antiparasitic dose of 200 µg/kg (Anonymous, 2020b). This dose rate provides a wide margin of safety (Guzzo et al., 2002). Adverse Drug Effects in humans occur with dose rates much higher than those prescribed in the Summary of Product Characteristics (SPC) of the marketing authorisation. A recent meta-analysis indicated that a dosage of 800 µg/kg was well-tolerated in patients with parasitic infections (Navarro et al., 2020) and more than 2.5 billion doses of IVM have been distributed over the last 30 years (Chaccour et al., 2020). It can therefore be anticipated that IVM, promoted through various media, may be used not only off-label, but also at doses significantly higher than those recommended for antiparasitic effects as recently suggested (Camprubí et al., 2020), in an attempt to achieve, *in vivo*, the virucidal concentrations obtained *in vitro*.

Obesity is a pathological condition which can significantly alter the pharmacokinetics of drugs (Cheymol, 2000) thus requiring dose adjustments (Knibbe et al., 2015). The avermectins are lipophilic, IVM XLogP3-AA = 4.1 as well as is the structurally related MOX (XLogP3-AA = 4.3), with an endectocidal profile similar to that of IVM

(Prichard et al., 2012) and recently licensed in humans for the treatment of onchocerciasis. Potentially, these drugs may require adjustments of dose in treating COVID-19. It is established that obesity is a major risk factor for COVID-19 (Williamson et al., 2020) with higher risks for hospitalization, admission to intensive care units and mortality (Popkin, Du, et al., 2020). Exacerbation of signs and symptoms of COVID-19 occurs through several mechanisms, including impaired immunity, chronic inflammation and increased proneness to blood clotting (Wadman, 2020b). Another negative effect of obesity is potential disruption of the Blood Brain Barrier (BBB). This has been reported in obese humans and animals with high fat diets (Rhea et al., 2017). Normally, IVM and MOX are safe as they do not penetrate the BBB, due to restriction by the P-glycoprotein (P-gp) efflux transporter (Schinkel et al., 1994) (Ménez et al., 2012). However, when BBB is disrupted, IVM penetration into the brain is potentially increased, leading to neurotoxicity through drug binding to central GABA-gated receptors (Chandler, 2018) (Baudou et al., 2020).

In this report, we document the effect of obesity on the disposition of IVM and MOX and additionally on a third avermectin, eprinomectin (EPR) (XLogP3-AA = 3.8) in a canine model of dietary obesity (Rocchini et al., 1987). Whilst EPR is not licensed in humans, it is used extensively in veterinary medicine. It is included in this evaluation, as there is considerable evidence of self-medication and self-dosing with veterinary products in COVID-19 subjects (Momekov & Momekova, 2020). This has led the USA Food and Drug Administration (FDA) to strongly discourage self-medication with avermectins intended for animals (Solomon, 2020). The data used in this report was previously presented as a meeting abstract (Bargues et al., 2009) and as a pharmacy thesis (Bargues, 2011).

## **MATERIALS AND METHODS**

The data generated by Bargues (Bargues, 2011) has been reanalyzed. The study was conducted in 7 female beagle dogs, aged 2-years and weighing 10.4±0.9 kg at trial commencement. They were housed in pairs in large cages in kennels of the Veterinary School of Toulouse. Each dog received an intravenous bolus of a drug combination, containing 66 µg/kg of each of three drugs, IVM, MOX and EPR, before (first period, control status) and again after (second period, obese status) 4-months on a high fat diet. Dogs were fed once daily and daily feed consumption recorded.

During the control period, dogs were fed a commercial pet chow diet (Croquettes Royal Canin Adulte Medium, Aimargues, France); this provided an energy supply of 3930 KCal/kg. The food ration (approximately 150g per dog) was calculated according to the maintenance energy needs with the formula  $130 * BW^{0.75}$  KCal adjusted to maintain a stable weight. For the second period, a dog chow of higher calorific value was provided (Croquettes Eukanuba Puppy Junior Aliment sec, Iams France, Neuilly sur Seine, France) with an energy content of 4500 KCal/kg. In addition, raw beef fat (8,500 KCal/kg) was given to provide an overall energy feed supply of 6100 KCal/kg, comprising 60% by the commercial chow and 40% by the beef fat. The objective of doubling the energy content of the ration in the second period was to increase body weight by 40% and to maintain it at this level throughout the second period. The fattening period was of 4 months duration. In both periods, dogs were weighed twice in each week. One adipolysis episode was induced by food restriction at 10 days (D) after administration of the test articles, *i.e.* between D10 and D15 for the first and the second period and from D26 to D31 only for the second period. For the first two days of each of these episodes, dogs were fasted and, for the three subsequent days, they received 50 g of the dog chow used during the control period.

Body Score Condition and body mass indices were measured according to those used to diagnose obesity in dogs in normal veterinary practice (Mawby et al., 2004). The percentage of body fat was evaluated using equations incorporating abdominal circumference and the length of the kneecap-tip of the calcaneus (Bargues, 2011). Body composition was also determined using the deuterium dilution technique for control and obese status. A 99.98% deuterium oxide solution (SigmaR, L'Isle d'Abeau Chesnes, La Verpillière, France) was administered at a dosage of 0.2 g/kg intravenously by catheter in the cephalic vein. Blood samples were obtained from the jugular vein (5 mL into heparinized tube) at times of 15, 30, 60, 90, 120, 150, 180 minutes post-administration. Plasma was harvested by centrifugation and stored at -80°C prior to analysis. Samples were analyzed for deuterium by mass spectrophotometry at the Aberdeen Center for Energy Regulation and Obesity (Aberdeen) laboratory (Król & Speakman, 1999).

A solution of IVM (Ivomec®, 1% solution for injection for cattle, Merial, France), EPR (Sigma, France) and MOX (Cydectin®, solution 1% injection for cattle, Fort Dodge),

in a volume of approximately 2 mL, was prepared in an intralipid buffer solution. The buffer solution was prepared from dog serum and a lipid emulsion (intralipid 20%, Fresenius Kabi) 200v/v; this ensured dissolution of the test article *in vivo*.

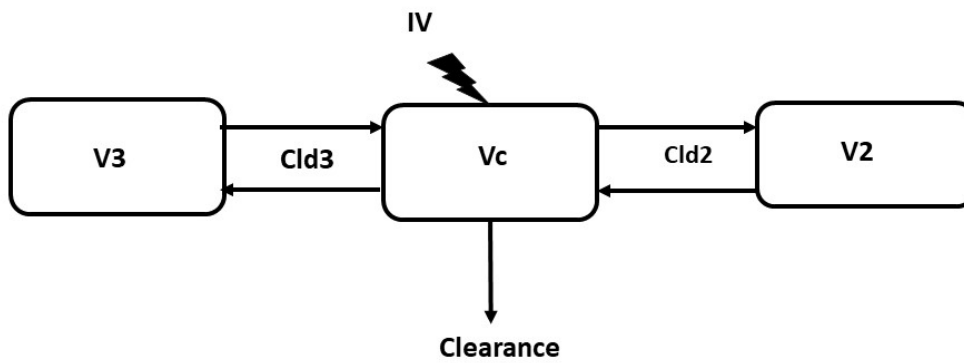
Administration was via a cephalic vein catheter. The dose rate of each substance was 66 µg/kg. The total dose was 198 µg/kg. The commonly used therapeutic dose of IVM, for treatment of parasitic infections in target species is 200 µg/kg. Blood samples (5 mL) were collected into heparinized tubes by direct puncture from the jugular vein, before administration and at 5, 15, 30 minutes after administration, then at 1, 2, 4, 8, 12 hours and 1, 2, 3, 4, 6, 8, 10, 11, 11.5, 12, 12.5, 13, 13.5, 14, 14.5, 15, 15.5, 18, 21, 28, 35, 42 and 53 days after administration. A further sample, 63 days after administration, was taken in the second period in obese dogs. Samples were centrifuged and plasma frozen at -20°C. The assays of MOX, IVM, EPR and the principal metabolite of IVM, 3-O-demethyl-ivermectin, were conducted using validated HPLC-fluorescence detection methods (Alvinerie et al., 1995), (Sutra et al., 1998). The lower limit of quantification for the three analytes was 0.1 ng/L. The coefficients of variations for intra-day precision ranged from 3.0 to 7.8% for MOX and from 0.4 to 9% for IVM and its metabolite. The coefficients of variation for inter-day precision were 5.3% for MOX and 5.7% for IVM and its metabolite.

### **Data analysis**

Pharmacokinetic modeling was carried out using commercially available software (Phoenix NLME version 8.3, Certara, St. Louis MO, United States). In a first step, each data set for each dog was individually analyzed by non-compartmental analysis (NCA) using the model 200-202, with dose expressed by BW (i.e. 66µg/kg). In a second step, all pairs of data sets for each test article were analyzed using a Nonlinear Mixed Effects (NLME) approach to generate population pharmacokinetic parameter estimates. For this analysis, the dose was not scaled by BW. Two- and three-compartment models were evaluated to identify the model that best described the data-set. The two models were compared using the likelihood ratio test and the 3-compartment model was selected. Parameterization was in terms of plasma clearance (CL), inter-compartmental clearance(s) (Cld) and volume(s) of distribution (V), with Vc, V2, V3, CL, Cld2 and Cld3 being the primary estimated parameters (figure 1). The following parameters were computed as secondary parameters,

namely the steady-state volume of distribution ( $V_{ss}$ ) with  $V_{ss}$  being the sum of  $V_c$ ,  $V_2$  and  $V_3$ , the mean residence time (MRT) as the ratio of  $V_{ss}$  and clearance and the terminal half-life computed from clearance and volume terms (Dubois et al., 2011).

**Figure 1:** The 3-compartmental model.  $V_c$ ,  $V_2$  and  $V_3$  are the volumes of distribution of the central, superficial and deep peripheral compartments, respectively.  $Cl_{d2}$  and  $Cl_{d3}$  are the distribution clearance for the superficial and deep compartment, respectively.



The between-subject variability (BSV) was modeled using an exponential model, and hence the clearance for the  $i^{th}$  subject was written as:

$$Cl_i = \theta_{median} \times \exp(\eta_i) \quad \text{Eq: 1}$$

Where  $Cl_i$  is the clearance for one of the test article in the  $i^{th}$  animal,  $\theta_{median}$  is the population median clearance (typical value of clearance) and  $\eta_i$  the deviation (noted ETA) associated with the  $i^{th}$  animal from the corresponding  $\theta_{median}$  population value. Other individual parameters (i.e.,  $V_c$ ,  $V_2$ ,  $V_3$  and  $Cl_{d2}$ ,  $Cl_{d3}$ ) were modeled using equations of the same form. The distribution of the ETAs was assumed normal with a mean of 0 and a variance ( $\omega_x^2$ ). In addition, the individual parameters and consequently their corresponding ETAs can be correlated. All these correlations were estimated and the corresponding covariances were stored in the variance-covariance omega matrix. The following equation 2 was used to convert the

variance ( $\omega_{clearance}^2$ ) of the log-transformed clearances into a coefficient of variation (CV %) in the original scale:

$$CV_{clearance}(\%) = 100 \times \sqrt{\exp(\omega_{clearance}^2) - 1} \quad \text{Eq: 2}$$

The shrinkage of random effects toward the means was calculated for the ETAs (Savic & Karlsson, 2009) with equation 3:

$$shrinkage = 1 - \frac{SD(EBE_{\eta})}{\omega} \quad \text{Eq: 3}$$

Where  $\omega$  is the estimated variability for the population and SD is the standard deviation of the individual values of the empirical Bayesian estimates (EBE) of  $\eta$ .

The residual model was an additive plus a multiplicative (proportional) model of the form:

$$C(t) = f(\theta, Time) \times (1 + \varepsilon_1) + \varepsilon_2 \quad \text{Eq: 4}$$

With  $\varepsilon_1$  and  $\varepsilon_2$ , the multiplicative and additive error terms having a mean of 0 and a variance noted  $\sigma_1$  or  $\sigma_2$ , respectively. The additive sigma is reported as its standard deviation with the same units as serum concentration (ng/mL) and the multiplicative sigma as the corresponding coefficient of variation.

Parameter estimation was based on minimizing an objective function value (OFV), using maximum likelihood estimation given for each model. A Laplacian engine was used for analyses approximating the marginal likelihood, while searching for the maximum likelihood. There were no censored data. A bootstrap approach was used to estimate typical values of parameters and precision of estimates that are reported by their 95% confidence intervals. To evaluate the overall performance of the final model, a Visual Predictive Check was plotted to compare actual observations with simulated replicates from the model (500 replicates per investigated dogs). The 90% prediction intervals were constructed and plotted together with the observed data allowing for a visual assessment of the agreement between simulation and observation. Diagnostic plots, the distribution of errors, and the precision of the parameter estimates were used as tools to evaluate the goodness of fit and to compare models.

The pivotal hypothesis of the analysis was that obesity was the covariate able to influence pharmacokinetic parameters and an analysis with the dogs status as covariate (control vs. obese) was carried out to evaluate its significance with (Eq: 5):

$$Param = \theta_{median} \times \exp(\theta_1 \times X_1) \text{ Eq: 5}$$

where *Param* is one of the structural parameters of the disposition model (Vc, V2, V3, CL, Cld2, Cld3),  $X_1$  is an indicator variable with a value of 0 for control condition and of 1 for obesity and  $\theta_1$ , the fixed effect of the covariate. For example, for VC, the model was given either by Eq 6 for the control condition, or Eq 7 for the obese condition:

$$Vc = \theta_{Vc_{median}} \times \exp(\eta Vc) \text{ Eq: 6}$$

$$Vc = \theta_{Vc_{median}} \times \exp(\theta_1) \times \exp(\eta Vc) \text{ Eq: 7}$$

where  $\theta_{Vc_{median}}$  is the typical value of Vc,  $\eta Vc$  is the ETAs associated with Vc and  $\theta_1$ , the fixed effect of the covariate for the obesity condition. If  $\theta_1$  is significantly different from zero, it provides evidence that a difference exists between the control and obese condition for Vc. No attempt was made to explore other covariates.

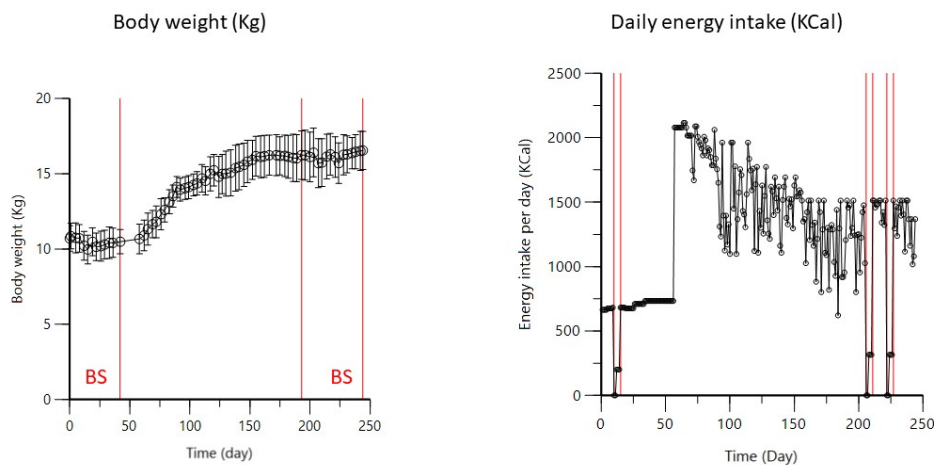
As there was a single covariate, the Phoenix Shotgun approach was used to evaluate all 64 possible scenarios (combination of parameters influenced or not by the covariate) to rank them using the Bayesian information criterion (BIC). A step-wise covariate search mode was also used to define the statistical significance of the covariate for each of the structural parameters of the model. This run mode performs a step-wise forward or backward addition or deletion of covariate effects (by adding/deleting one at a time) to determine the improvement of the final model based on the BIC. For the present analysis, we selected a BIC value of 6.635 for adding a covariate and a value of 10.823 for deleting the covariate.

## Results

Figure 2 depicts the time development of the average BW (kg) and caloric intake for the 7 dogs. During the first period, the average BW was  $10.4 \pm 0.9$  kg (min-max: 8.1 - 12.1 kg) and the energy requirements, maintaining this stable control BW,

amounted to approximately 750 Kcal/day. The fattening ration provided excess caloric intake throughout the duration of the high fat diet. When the weight stabilization phase was reached (approximately 100 days after the start of fattening, i.e. on D150), the percentage weight gain was  $57 \pm 25\%$  ( $P < 0.01$ ). The obesity status, defined as 20% weight gain over normal weight, was largely achieved. As during the first blood sampling period, BW of the dogs was stable during the second sampling period, ranging from to  $15.2 \pm 1.7$  kg (min-max: 13.6 - 18.9 kg).

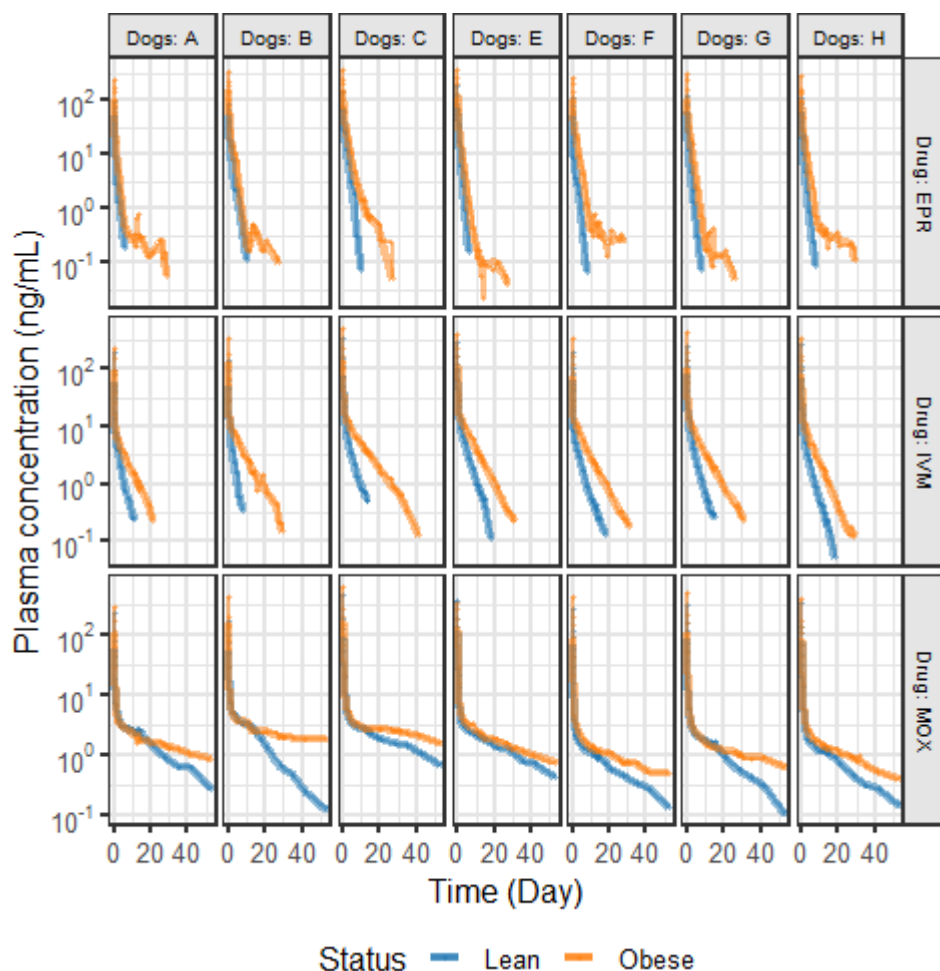
**Figure 2: left panel:** Time development (days) of body weight (kg) (mean and SD) for the 7 dogs. Red vertical lines indicate time of blood sampling (BS) during the first (lean) and second period (obese); **Right panel:** average daily caloric intake (Kcal) for the 7 dogs during the study. Red vertical lines indicate episode of energy intake restriction (10-15, 206-211 and 222-227 days)



The percentages of body fat (mean and SD) calculated from the body mass index, during the first and second periods, were  $24.6 \pm 4.6\%$  and  $38.2 \pm 2.6\%$ , respectively ( $P < 0.01$ ). Using the deuterium oxide dilution technique, the average body fat percentage was  $21.9 \pm 3.3\%$  (range 15.9%-23.8%) in the first period and  $43.7 \pm 2.3\%$  (range 39.9%-46.1%) in the second ( $P < 0.01$ ). The high fat diet produced an increase in body fat percentage of  $104 \pm 41\%$ .

Individual plots for each test article and each dog, before and after, fattening are depicted in figure 3. Visual inspection indicates that obesity exerted a large effect on the disposition of IVM, MOX and EPR, with much slower elimination for each test article during the period of obesity.

**Figure 3:** Semi-logarithmic plots of the disposition curves of IVM, MOX and EPR after a single administration of each drug as a cocktail at the dose rate of 66 µg/Kg by IV injection in 7 dogs in control (blue curves) and obesity (orange curves) conditions.



### Non-compartmental analysis

Results of the NCA are presented in table 1.

**Table 1:** Results of the NCA analysis (Model 200-202, Log-linear trapezoidal rule) for the three drugs and 7 dogs

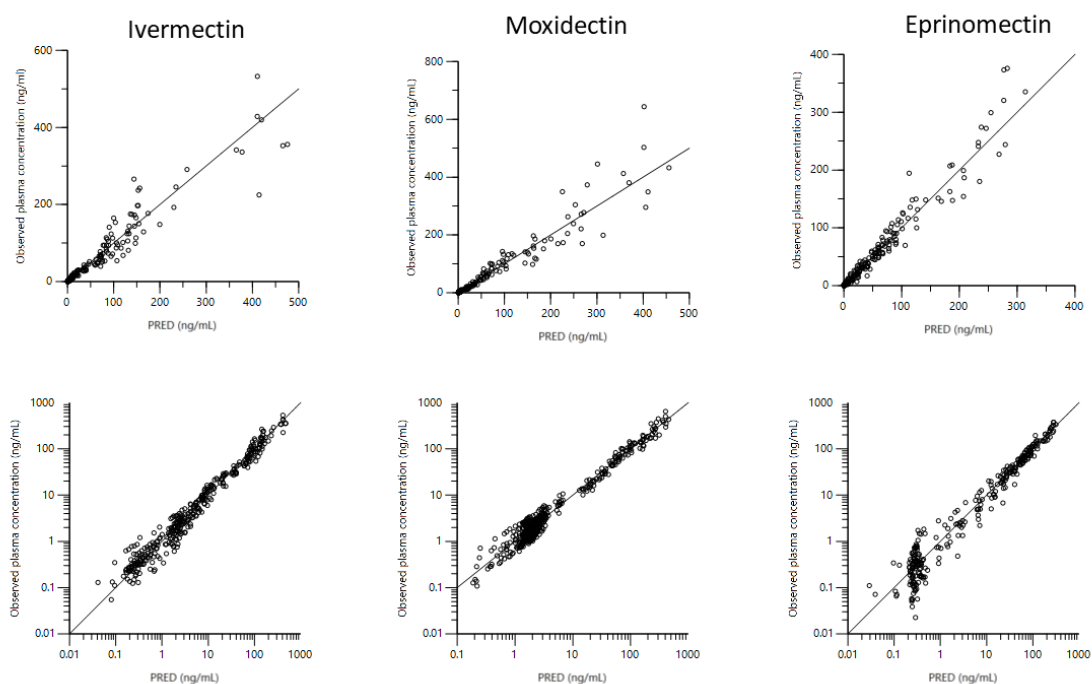
Parameters (units)	Substance	Status	Mean	SD	Variation (%)	P value
Clearance (mL/Kg/day)	IVM	Lean	1290	393		
	IVM	Obese	583	178	-55%	0.001
	MOX	Lean	748	249		
	MOX	Obese	431	174	-42%	0.001
	EPR	Lean	1503	387		
	EPR	Obese	552	159	-63%	0.0001
Vss (mL/Kg)	IVM	Lean	2951	583		
	IVM	Obese	3124	546	+6%	NS
	MOX	Lean	10917	2705		
	MOX	Obese	15079	2772	+38%	0.0171
	EPR	Lean	1751	388		
	EPR	Obese	1246	341	-29%	0.0190
MRT (day)	IVM	Lean	2.38	0.51		
	IVM	Obese	5.57	0.95	+134%	0.001
	MOX	Lean	15.40	4.23		
	MOX	Obese	40.62	20.56	+164%	0.027
	EPR	Lean	1.21	0.30		
	EPR	Obese	2.31	0.46	+91%	0.001
Half-life (day)	IVM	Lean	2.47	0.75		
	IVM	Obese	4.36	0.37	+76%	0.032
	MOX	Lean	13.68	3.45		
	MOX	Obese	35.63	13.71	+161%	0.013
	EPR	Lean	0.99	0.16		
	EPR	Obese	3.03	1.05	+206%	0.0029
Vz (mL/Kg)	IVM	Lean	4508	1525		
	IVM	Obese	3637	1044	-19%	NS
	MOX	Lean	14471	5357		
	MOX	Obese	19924	4494	+38%	0.015
	EPR	Lean	2140	662		
	EPR	Obese	2426	1084	+13%	NS

*Clearance: plasma clearance; Vss: steady-state volume of distribution; MRT: Mean Residence Time computed with extrapolation to infinity. Half-life: terminal half-life; Vz: Volume of distribution associated with the terminal phase. P values obtained with a paired t test.*

For the three test articles, plasma clearance, expressed per kg BW, was significantly decreased (by 55, 42 and 63% for IVM, MOX and EPR, respectively) during the obesity period. This was associated with large increases in MRT (134, 164 and 91% for IVM, MOX and EPR, respectively) and terminal half-life (76, 161 and 206% for IVM, MOX and EPR, respectively) For volume of distribution, there was no significant difference for IVM, an increase for MOX (38%) and a decrease for EPR (29%). Similarly, for Vz (i.e. Varea) a parameter associated with the terminal phase, there were no differences for IVM and EPR, while it was significantly increased by MOX (38%) P=0.015.

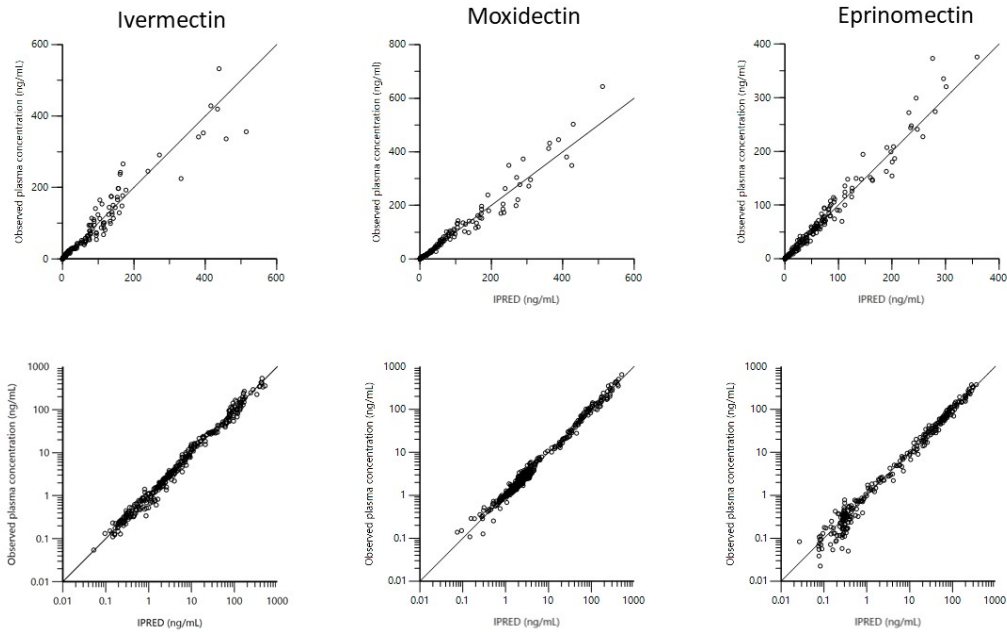
In a second step, a compartmental analysis, using a 3-compartmental approach, was used. Figures 4 to 6 are Goodness-of-fit (GOF) plots supporting the 3-compartmental structural model, the exponential model for the random component and the additive plus multiplicative model for the error sub-model used to analyse the data.

**Figure 4:** Plots of the dependent variable i.e. of observed plasma concentrations (ng/mL) versus population predicted plasma concentrations (PRED) (no random component) for the three drugs. The plots illustrate observed vs. fitted values of the model function. Ideally they should fall close to the line of unity  $y=x$ . Arithmetic scale (upper) and logarithmic scale (lower).



*For both arithmetic and logarithmic scales, data are evenly distributed about the line of identity, indicating no major bias in the population component of the model.*

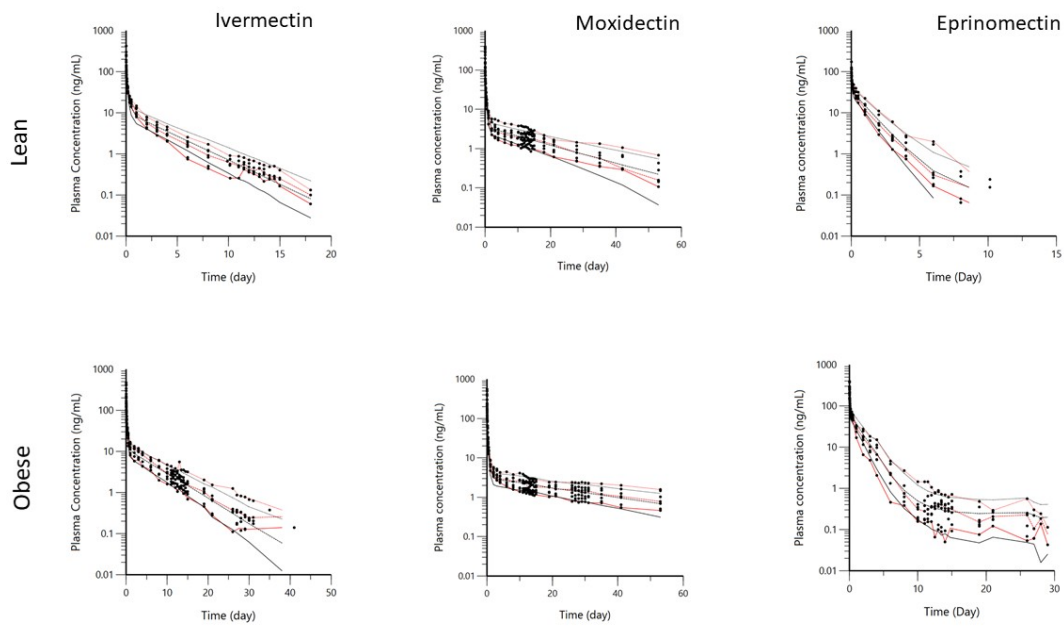
**Figure 5:** Plots of the dependent variable, observed plasma concentrations (ng/mL), versus individual predicted plasma concentrations (IPRED) for the three drugs. Individual predictions were obtained by setting random effects to the 'post hoc' or Empirical Bayesian Estimate of the random effects for the individual dog, from which the plasma concentration observation was made. Thus, the plot illustrates observed vs. fitted values of the model function. Ideally, they should fall close to the line of unity  $y=x$ . Arithmetic scale (upper) and logarithmic scale (lower).



*For both arithmetic and logarithmic scales, data are evenly distributed about the line of identity, indicating no major bias in the population component of the model*

The adequacy of the 3-compartmental was checked by plotting the Visual Predictive Check (VPC). The 10th, 50th and 90th percentiles of the simulated distribution were compared to the observations. A binning option (K-means) was used.

**Figure 6:** Visual Predictive Check (VPC) obtained with 500 replicates of each dog and each status (lean, obese). For each stratification, the observed quantiles (10, 50 and 90%) were well super-imposed with the corresponding predictive check quantiles over the observed data. Red lines: observed quantiles; Black lines: predicted quantiles; Black symbols: observed data.



Typical values of the primary structural parameters of the model (thetas), the secondary parameters (MRT, Vss, half-life....), their associated CV% and the SD of the residuals are presented in Tables 2 and 3.

**Table 2:** Population primary parameters as obtained with a 3-compartment model with covariate (COV) (lean vs. obese); estimates bootstrap 2.5% and 97.5% percentiles.

Parameters	Unit	IVM			MOX			EPR		
		Tv	2.5% CI	97.5% CI	Tv	2.5% CI	97.5% CI	Tv	2.5% CI	97.5% CI
tvVc (lean)	L	0.078	0.054	0.140	2.232	1.818	2.559	6.499	5.244	7.459
tvV2 (lean)	L	3.46	2.96	4.12	6.38	5.81	7.01	10.34	9.47	11.37
tvV3 (lean)	L	24.47	21.15	27.51	103.37	80.64	124.89	1.40	0.67	15651.93
tvClearance (lean)	L/day	11.37	10.09	12.86	7.76	6.28	9.06	15.00	4.94	36.65
tvCld2 (lean)	L/day	62.88	45.97	97.36	115.85	98.03	126.97	89.95	74.60	121.58
tvCld3 (lean)	L/day	17.88	16.73	19.57	22.50	19.34	26.24	0.85	-21.68	14.82
COV Clearance	scalar	-0.266	-0.348	-0.170	0.000	0.000	0.000	0.811	-1.427	1.260
COV Cld2	scalar	0	0	0	0	0	0	0	0	0
COV Cld3	scalar	0	0	0	0.167	0.078	0.266	0.880	-2.010	6.812
COV Vc	scala	0	0	0	0.00	0.000	0.000	-	-0.763	-0.430

	r				0			0.56		
								0		
COV V2	scalar	0	0	0	0	0	0	0	0	0
COV V3	scalar	0.50	0.359	0.697	0.681	0.426	0.988	5.043	-3.720	5.925
tvV3 (obese)	L	40.35	30.27	55.25	204.17	123.41	335.54	217.29	0.02	5860201.29
tvClearance (obese)	L/day	8.72	7.12	10.85	7.76	6.28	9.06	6.67	1.19	129.16
error (multiplicative)	CV%	21.85	24.14	18.02	17.17	17.59	15.34	18.68	30.33	14.30
error (additive) stdev0	ng/mL	0.001	0.001	0.001	0.072	0.001	0.120	0.112	0.011	0.210

*V<sub>c</sub>: volume of the central compartment; V<sub>2</sub>: volume of the shallow peripheral compartment; V<sub>3</sub>: volume of the deep peripheral compartment, Cl: plasma clearance; Cl<sub>d2</sub> and Cl<sub>d3</sub>: distribution clearance for the shallow and deep compartment ; multiplicative component of the error model is expressed as CV% and the additive component of the residual error model by its standard deviation. tv lean : typical values for the control status (lean) ; COV are the estimate of the fixed effect for covariates (exponential model). tv obese are typical value for the obese status; it is obtained by the product of the tv lean by the exponential of the corresponding scalar (e.g. the tv of clearance for IVM for obese condition is 11.37 L/day fold exp(-0.266) equal to 8.72 L/day. Confidence interval of the different estimates were obtained using bootstrap sampling. For EPR, despite the 3-compartmental model was the best in terms of AIC, structural parameters of the third compartment (V<sub>3</sub> and Cl<sub>d3</sub>) were poorly estimated as well as corresponding covariates. The average BW was 10.4 ± 0.9 kg (min-max: 8.1 - 12.1 kg) during the lean period vs 15.2 ± 1.7 kg (min-max: 13.6 - 18.9 kg) during the obesity period.*

Data in table 2 indicate that clearances, expressed in absolute values, were either not significantly modified (MOX) or even reduced in obese dogs (IVM). For EPR, there was also a reduction in clearance but the covariate was poorly estimated and the results should be interpreted with caution. The volume of the deep compartment (V<sub>3</sub>) was increased for the three drugs but again with poor precision for EPR.

**Table 3:** Population secondary parameters obtained with a 3-compartments model with covariate (COV) (lean vs. obese); estimates were obtained from typical values of primary parameters of table 2.

		IVM	MOX	EPR
Vss lean	L	28.01	111.98	18.24
Vss obese	L	43.89	213.94	230.95
MRT lean	Day	2.46	14.44	1.22
MRT obese	Day	5.03	27.59	34.64
HL lean	Day	2.58	13.00	1.31
HL obese	Day	4.85	24.16	96.38

*Vss: steady-state volume of distribution; MRT: Mean Residence Time (MRT); HL: terminal Half-life. For HL, the calculated parameters for obese status were poorly estimated in terms of precision and the figures for this status should be viewed with*

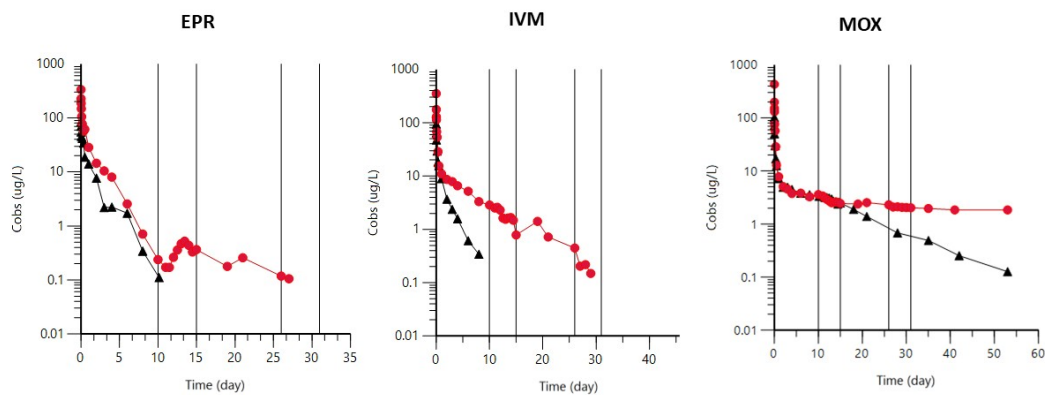
*caution. The average BW was  $10.4 \pm 0.9$  kg (min-max: 8.1 - 12.1 kg) during the lean period vs  $15.2 \pm 1.7$  kg (min-max: 13.6 - 18.9 kg) during the obesity period.*

Inspection of table 3 shows that  $V_{ss}$  was significantly increased in the obesity condition for the three drugs, accounting for the corresponding increase in MRT.

The between-subject variability (BSV) for clearance was 20.0, 30.9 and 24.01 %, respectively, for IVM, MOX and EPR. For  $V_3$ , the deep compartment, BSV was relatively small for IVM and MOX (8.4 and 6.84%) but very high for EPR (153%). This was due to the fact that the third phase was not clearly identified in all dogs (see figure 2).

In the present experiment, we induced in dogs a first episode of fasting (two days) followed by three days of restriction of energy intake 10 days after drug administration and, only during the obesity status, a second fasting episode 26 days after drug administration. This protocol was designed to investigate the effects of lipomobilization on plasma concentrations of the three drugs studied. A clear rebound was obtained only for EPR during the first episode of fasting and only in obese dogs. No such rebound occurred with IVM and MOX (figure 7).

**Figure 7:** Effect of a 2-day fasting episode followed by a 3-day caloric restriction triggered 10 days (lean dog, black dots) or 10 and 26 days (obese dog, red dots) after administration of EPR, IVM and MOX on plasma concentrations of each drug in a representative dog (dog B). Vertical lines indicate episodes of fasting (2 days) followed by caloric restriction (3 days)



## Discussion and conclusions

Conditions of overweight/obesity occur with a prevalence greater than 20% in almost all countries (Popkin, Du, et al., 2020) (Popkin, Corvalan, et al., 2020). Currently, 32% of people in the United States are overweight (Wadman, 2020a). Obesity is a classical co-morbid factor for several diseases, including hypertension, cardiovascular disease, dyslipidemia, type-2 diabetes... and it was also recently reported for COVID-19. Of almost 17,000 patients hospitalized in USA with COVID-19, were either overweight (29%) or obese (48%) (Rizzo et al., 2020). IVM is widely used worldwide and the administrated dose is usually based on the patient body weight. The lack of specific dosing guidelines for this drug in obese subjects is partly attributable to the *a priori* exclusion of obese subjects from clinical trials (Han et al., 2007). Given the attention paid recently to IVM in the prevention and treatment of COVID-19 and in view of its lipophilic nature, the present study provides some preliminary data on which to base possible adaptation of dosage in obese patients in general but in particular those affected with COVID-19. The most appropriate way to address this question would be to conduct population pharmacokinetic studies in the target patients receiving IVM or MOX. However, the results of such studies are not currently available, yet there is current urgency deriving from the COVID-19 situation. Moreover, there are no universal guidelines for adjusting dosages in cases of obesity (Green & Duffull, 2004). Data from the model used in this study of obesity in dogs provides initial first steps towards a more definitive answer.

The dog as a species provides a good comparative model for human obesity, since clinical signs are similar in the two species (Osto & Lutz, 2015). The obesity model used in this study was initially developed to study hypertension (Rocchini et al., 1987) (Verwaerde et al., 1999) and it has been used also in pharmacokinetic investigations because of its ability to rapidly achieve relatively severe obesity and its reversibility. The model has several similarities with human obesity as occurring in hyperinsulinemia and insulin resistance (Rocchini et al., 1987).

The experimental design has enabled use of the same dogs to study the two conditions, control and obese, and the combination/simultaneous drug dosing schedule ensured good discriminative power. The design also allowed comparison of both the influence of obesity on the disposition of the three investigated drugs and generated data indicating differences between them, each drug having its own unique physico-chemical properties. The study also minimized the numbers of animals used experimentally. For IVM and MOX, the data generated for control dogs was in agreement with previously reported findings for IVM (Lo et al., 1985) and MOX (Lallemand et al., 2007). In the latter studies, each drug was administered alone, and this validates drug combination dosing, as indeed it has also been validated for many other compounds (He et al., 2008).

The principal finding from this study is that, in obese dogs, the clearance of the three investigated drugs, expressed in absolute values (L/day), was either not modified (MOX) or reduced (IVM and EPR). The consequence was a significant decrease in clearance when scaled by actual body weight (-42%, -55% and -63% for MOX, IVM and EPR, respectively). This is in line, at least for MOX, with previous reports which demonstrated that the clearance (expressed in absolute value) of several drugs, including phenazone, carbamazepine, lithium, remifentanyl, cefazolin, and theophylline, was not influenced by obesity (Mahmood, 2012).

In human medicine, recommended oral dosage of IVM and MOX is weight-based, on the assumption that plasma clearance is directly proportional to TBW, regardless of body composition. In practice, this means that the same dose level will be administered to a tall lean subject and a small obese subject of the same TBW. Assuming that obesity does not alter the oral bioavailability (Hanley et al., 2010) (Knibbe et al., 2015), the present trial suggests rather that, in obese subjects, the

actual BW should not be considered in computing a maintenance dosage for IVM or MOX. Indeed, clearance and bioavailability are the only pharmacokinetic parameters controlling internal exposure, and the total clearance of the three drugs reported in this study was unchanged or even decreased in obesity, compared to clearance in lean animals. It is concluded that the same total dose should be considered to lean and obese subjects, regardless of their actual BW and dose should be computed on a LBW basis, not a TBW. This is supported by conclusions reached by others, namely that LBW suffices to explain the influence of body composition on clearance and can therefore adequately predict drug exposure in the obese subjects (Han et al., 2007). The underlying rationale is that 99% of the body's metabolic processes (including clearance) takes place in lean tissues (Han et al., 2007).

An additional finding of clinical significance is the large increase in the absolute value (L) of volume of distribution in obesity especially that of the deep compartment (V<sub>3</sub>), as evidenced by compartmental analysis. This supports the hypothesis that V<sub>3</sub> represents the adipose tissue, for which IVM, MOX and EPR display a large affinity. This results in increased MRT and terminal half-life, because these two time parameters are hybrids; they depend on both clearance and volume of distribution (V<sub>ss</sub> for MRT, V<sub>area</sub> or V<sub>z</sub> for half-life) (Toutain & Bousquet-Melou, 2004). The practical consequence is a possible greater accumulation of the drugs, with repeated administrations and a longer lag-time to reach a state of equilibrium ensuring the same internal exposure as for the lean counterpart. The delay is approximately three-fold the terminal half-life (and MRT) and it is increased two-fold in obesity for IVM and MOX. This leads to long delays from some 10 to 20 days for IVM and from 2 to 4 weeks for MOX in lean vs. obese subjects, respectively.

Given the length of these delays, and if rapid attainment of maximal effect is required, a loading dose could be considered and for this, the relevant pharmacokinetic parameter is V<sub>ss</sub>. The absolute value of the latter is doubled in obese subjects for both IVM and MOX. Therefore, the loading dose, for the same plasma concentrations at steady state, must be 2-fold greater in obese than in lean subjects, while the maintenance dose should be unchanged. Comparison of the weight-normalized circumstance, between obese and non-obese individuals, provides insights into how a drug distributes into excess weight (Hanley et al., 2010). When volume of distribution normalized by TBW is similar in obese and non-obese

subjects, as in this study, it can be concluded that the drugs exhibit marked sequestration in adipose tissue. Hence, a weight-based loading dose for such a drug is appropriate (Hanley et al., 2010). The present data are consistent with the opinion of Green and Duffull that, according to most published studies, TBW is the best descriptor of volume of distribution in obese subjects (Green & Duffull, 2004). Considering the numerical value of plasma clearance and V<sub>ss</sub>, it seems that, for a given therapeutic objective, the loading dose for MOX should be much higher than the maintenance dose. This is less the case for IVM. Therefore, it is likely that, if repeated doses are required, and all things being equal in terms of therapeutic objective, dose and dosing interval, IVM is a more convenient therapeutic choice than MOX.

COVID-19 is associated with clinically significant weight loss (Di Filippo et al., 2020) and, in the present experiment, a period of fasting (2 days) was followed by 3 days of restriction of energy intake to ascertain the effects of lipomobilization on plasma concentrations of the drugs studied. A rebound phenomenon occurred for EPR in the obesity condition. On the other hand, this was less marked for IVM and absent for MOX.

**In conclusion**, the present analysis suggests that, when daily dosing is required, the maintenance doses of IVM and MOX should not be adjusted for body weight in obese subjects; dosage should be based on LBW. On the other hand, determining a loading dose must take into account the actual BW and this loading dose will be significantly higher than the maintenance daily dose, especially for MOX, which makes MOX less attractive than IVM in case of repeated dosing. EPR, an avermectin not licensed for use in human medicine, behaves like IVM and offers no specific advantage over IVM and its off-label use in human medicine should be discouraged.

**Acknowledgements:** To Professor Peter Lees, Royal Veterinary College, University of London, for constructive criticism and editorial corrections.

**Data availability statement:** Data available on request from the authors

**Funding statement:** Not applicable

**Author contribution statement:** A. Bousquet-Mélou was responsible for the study

design and contributed to data analysis and interpretation. A. Lespine and JF Sutra were responsible for analytical quantification of the investigated substances. I Bargues conducted the animal phase and managed the data sets. P-L. Toutain contributed to data analysis and interpretation and he wrote the first draft of the manuscript. All co-authors made intellectual input into the study and critically reviewed several drafts of the manuscript.

**Conflict of interest disclosure:** no competing interests to declare.

**Ethics approval statement:** No specific animal experiments were carried out. The publication is based on a more advanced and focused analysis of data published in 2009 in the form of a Meeting Abstract and which was incorporated in a pharmacy thesis defended in 2011. All animal procedures were conducted in accordance with accepted standards of humane animal care required at that time under agreement number 31–242 for animal experimentation from the French Ministry of Agriculture.

## References

- Alvinerie, M., Sutra, J. F., Badri, M., & Galtier, P. (1995). Determination of moxidectin in plasma by high-performance liquid chromatography with automated solid-phase extraction and fluorescence detection. *Journal of Chromatography. B, Biomedical Applications*, 674(1), 119–124. [https://doi.org/10.1016/0378-4347\(95\)00294-5](https://doi.org/10.1016/0378-4347(95)00294-5)
- Anonymous. (2020a). *Clinicaltrials.gov*. <https://clinicaltrials.gov/ct2/results?cond=Covid19&term=ivermectin&cntry=&state=&city=&dist=>
- Anonymous. (2020b). *Stromectol (Ivermectin): Uses, Dosage, Side Effects, Interactions, Warning*. RxList. <https://www.rxlist.com/stromectol-drug.htm>
- Bargues, I. (2011). *INFLUENCE DE L'OBESITE SUR LES PARAMETRES PHARMACOCINETIQUES DE TROIS SUBSTANCES ANTIPARASITAIRES LIPOPHILES [POUR LE DIPLOME D'ETAT DE DOCTEUR EN PHARMACIE]*. UNIVERSITE TOULOUSE III – Paul SABATIER FACULTE DES SCIENCES PHARMACEUTIQUES.

- Bargues, I., Lespine, A., Toutain, P. L., & Bousquet-Melou, A. (2009). Influence of obesity on the pharmacokinetics of anthelmintic macrocyclic lactones in dogs. *JOURNAL OF VETERINARY PHARMACOLOGY AND THERAPEUTICS*, 32, 161–162.
- Baudou, E., Lespine, A., Durrieu, G., André, F., Gandia, P., Durand, C., & Cunat, S. (2020). Serious Ivermectin Toxicity and Human *ABCB1* Nonsense Mutations. *New England Journal of Medicine*, 383(8), 787–789.  
<https://doi.org/10.1056/NEJMc1917344>
- Bray, M., Rayner, C., Noël, F., Jans, D., & Wagstaff, K. (2020). Ivermectin and COVID-19: A report in Antiviral Research, widespread interest, an FDA warning, two letters to the editor and the authors' responses. *Antiviral Research*, 178, 104805. <https://doi.org/10.1016/j.antiviral.2020.104805>
- Caly, L., Druce, J. D., Catton, M. G., Jans, D. A., & Wagstaff, K. M. (2020). The FDA-approved drug ivermectin inhibits the replication of SARS-CoV-2 in vitro. *Antiviral Research*, 178, 104787.  
<https://doi.org/10.1016/j.antiviral.2020.104787>
- Camprubí, D., Almuedo-Riera, A., Martí-Soler, H., Soriano, A., Hurtado, J. C., Subirà, C., Grau-Pujol, B., Krolewiecki, A., & Muñoz, J. (2020). Lack of efficacy of standard doses of ivermectin in severe COVID-19 patients. *PLOS ONE*, 15(11), e0242184. <https://doi.org/10.1371/journal.pone.0242184>
- Chaccour, C., Hammann, F., Ramón-García, S., & Rabinovich, N. R. (2020). Ivermectin and COVID-19: Keeping Rigor in Times of Urgency. *The American Journal of Tropical Medicine and Hygiene*, 102(6), 1156–1157. <https://doi.org/10.4269/ajtmh.20-0271>

- Chandler, R. E. (2018). Serious Neurological Adverse Events after Ivermectin—Do They Occur beyond the Indication of Onchocerciasis? *The American Journal of Tropical Medicine and Hygiene*, 98(2), 382–388.  
<https://doi.org/10.4269/ajtmh.17-0042>
- Cheymol, G. (2000). Effects of obesity on pharmacokinetics implications for drug therapy. *Clinical Pharmacokinetics*, 39(3), 215–231.  
<https://doi.org/10.2165/00003088-200039030-00004>
- Cupp, E. W., Sauerbrey, M., & Richards, F. (2011). Elimination of human onchocerciasis: History of progress and current feasibility using ivermectin (Mectizan®) monotherapy. *Acta Tropica*, 120, S100–S108.  
<https://doi.org/10.1016/j.actatropica.2010.08.009>
- Di Filippo, L., De Lorenzo, R., D'Amico, M., Sofia, V., Roveri, L., Mele, R., Saibene, A., Rovere-Querini, P., & Conte, C. (2020). COVID-19 is associated with clinically significant weight loss and risk of malnutrition, independent of hospitalisation: A post-hoc analysis of a prospective cohort study. *Clinical Nutrition*, S0261561420305896. <https://doi.org/10.1016/j.clnu.2020.10.043>
- Dubois, A., Bertrand, J., & Mentré, F. (2011). *Mathematical Expressions of the Pharmacokinetic and Pharmacodynamic Models implemented in the PFIM software*. UMR738, INSERM, University Paris Diderot.  
[http://www.pfim.biostat.fr/PFIM\\_PKPD\\_library.pdf](http://www.pfim.biostat.fr/PFIM_PKPD_library.pdf)
- Fox, L. M. (2006). Ivermectin: Uses and impact 20 years on. *Current Opinion in Infectious Diseases*, 19(6), 588–593.  
<https://doi.org/10.1097/QCO.0b013e328010774c>
- Green, B., & Duffull, S. B. (2004). What is the best size descriptor to use for pharmacokinetic studies in the obese? *British Journal of Clinical*

*Pharmacology*, 58(2), 119–133. <https://doi.org/10.1111/j.1365-2125.2004.02157.x>

Guzzo, C. A., Furtek, C. I., Porras, A. G., Chen, C., Tipping, R., Clineschmidt, C. M., Sciberras, D. G., Hsieh, J. Y.-K., & Lassetter, K. C. (2002). Safety, Tolerability, and Pharmacokinetics of Escalating High Doses of Ivermectin in Healthy Adult Subjects. *Journal of Clinical Pharmacology*, 42(10), 1122–1133.

<https://doi.org/10.1177/009127002401382731>

Han, P. Y., Duffull, S. B., Kirkpatrick, C. M. J., & Green, B. (2007). Dosing in Obesity: A Simple Solution to a Big Problem. *Clinical Pharmacology & Therapeutics*, 82(5), 505–508. <https://doi.org/10.1038/sj.clpt.6100381>

Hanley, M. J., Abernethy, D. R., & Greenblatt, D. J. (2010). Effect of obesity on the pharmacokinetics of drugs in humans. *Clinical Pharmacokinetics*, 49(2), 71–87. <https://doi.org/10.2165/11318100-000000000-00000>

He, K., Qian, M., Wong, H., Bai, S. A., He, B., Brogdon, B., Grace, J. E., Xin, B., Wu, J., Ren, S. X., Zeng, H., Deng, Y., Graden, D. M., Olah, T. V., Unger, S. E., Luettgen, J. M., Knabb, R. M., Pinto, D. J., Lam, P. Y. S., ... Grossman, S. J. (2008). N-in-1 Dosing Pharmacokinetics in Drug Discovery: Experience, Theoretical and Practical Considerations. *Journal of Pharmaceutical Sciences*, 97(7), 2568–2580. <https://doi.org/10.1002/jps.21196>

Heidary, F., & Gharebaghi, R. (2020). Ivermectin: A systematic review from antiviral effects to COVID-19 complementary regimen. *The Journal of Antibiotics*, 73(9), 593–602. <https://doi.org/10.1038/s41429-020-0336-z>

Knibbe, C. A. J., Brill, M. J. E., van Rongen, A., Diepstraten, J., van der Graaf, P. H., & Danhof, M. (2015). Drug Disposition in Obesity: Toward Evidence-Based

- Dosing. *Annual Review of Pharmacology and Toxicology*, 55(1), 149–167.  
<https://doi.org/10.1146/annurev-pharmtox-010814-124354>
- Król, E., & Speakman, J. R. (1999). Isotope dilution spaces of mice injected simultaneously with deuterium, tritium and oxygen-18. *The Journal of Experimental Biology*, 202(Pt 20), 2839–2849.
- Lallemand, E., Lespine, A., Alvinerie, M., Bousquet-Melou, A., & Toutain, P.-L. (2007). Estimation of absolute oral bioavailability of moxidectin in dogs using a semi-simultaneous method: Influence of lipid co-administration. *Journal of Veterinary Pharmacology and Therapeutics*, 30(5), 375–380.  
<https://doi.org/10.1111/j.1365-2885.2007.00878.x>
- Lo, P. K., Fink, D. W., Williams, J. B., & Blodinger, J. (1985). Pharmacokinetic studies of ivermectin: Effects of formulation. *Veterinary Research Communications*, 9(4), 251–268. <https://doi.org/10.1007/BF02215150>
- Mahmood, I. (2012). Prediction of clearance and volume of distribution in the obese from normal weight subjects: An allometric approach. *Clinical Pharmacokinetics*, 51(8), 527–542. <https://doi.org/10.2165/11631630-000000000-00000>
- Mawby, D. I., Bartges, J. W., d'Avignon, A., Laflamme, D. P., Moyers, T. D., & Cottrell, T. (2004). Comparison of various methods for estimating body fat in dogs. *Journal of the American Animal Hospital Association*, 40(2), 109–114.  
<https://doi.org/10.5326/0400109>
- Ménez, C., Sutra, J.-F., Prichard, R., & Lespine, A. (2012). Relative Neurotoxicity of Ivermectin and Moxidectin in Mdr1ab (–/–) Mice and Effects on Mammalian GABA(A) Channel Activity. *PLoS Neglected Tropical Diseases*, 6(11), e1883.  
<https://doi.org/10.1371/journal.pntd.0001883>

- Momekov, G., & Momekova, D. (2020). Ivermectin as a potential COVID-19 treatment from the pharmacokinetic point of view: Antiviral levels are not likely attainable with known dosing regimens. *Biotechnology & Biotechnological Equipment*, 34(1), 469–474. <https://doi.org/10.1080/13102818.2020.1775118>
- Navarro, M., Camprubí, D., Requena-Méndez, A., Buonfrate, D., Giorli, G., Kamgno, J., Gardon, J., Boussinesq, M., Muñoz, J., & Krolewiecki, A. (2020). Safety of high-dose ivermectin: A systematic review and meta-analysis. *The Journal of Antimicrobial Chemotherapy*, 75(4), 827–834. <https://doi.org/10.1093/jac/dkz524>
- Osto, M., & Lutz, T. A. (2015). Translational value of animal models of obesity-Focus on dogs and cats. *European Journal of Pharmacology*, 759, 240–252. <https://doi.org/10.1016/j.ejphar.2015.03.036>
- Popkin, B. M., Corvalan, C., & Grummer-Strawn, L. M. (2020). Dynamics of the double burden of malnutrition and the changing nutrition reality. *Lancet (London, England)*, 395(10217), 65–74. [https://doi.org/10.1016/S0140-6736\(19\)32497-3](https://doi.org/10.1016/S0140-6736(19)32497-3)
- Popkin, B. M., Du, S., Green, W. D., Beck, M. A., Algaith, T., Herbst, C. H., Alsukait, R. F., Alluhidan, M., Alazemi, N., & Shekar, M. (2020). Individuals with obesity and COVID-19: A global perspective on the epidemiology and biological relationships. *Obesity Reviews*, obr.13128. <https://doi.org/10.1111/obr.13128>
- Prichard, R., Ménez, C., & Lespine, A. (2012). Moxidectin and the avermectins: Consanguinity but not identity. *International Journal for Parasitology. Drugs and Drug Resistance*, 2, 134–153. <https://doi.org/10.1016/j.ijpddr.2012.04.001>

- Rhea, E. M., Salameh, T. S., Logsdon, A. F., Hanson, A. J., Erickson, M. A., & Banks, W. A. (2017). Blood-Brain Barriers in Obesity. *The AAPS Journal*, 19(4), 921–930. <https://doi.org/10.1208/s12248-017-0079-3>
- Rizzo, S., Chawla, D., Zalocusky, K., Keebler, D., Chia, J., Lindsay, L., Yau, V., Kamath, T., & Tsai, L. (2020). *Descriptive epidemiology of 16,780 hospitalized COVID-19 patients in the United States* [Preprint]. *Infectious Diseases (except HIV/AIDS)*. <https://doi.org/10.1101/2020.07.17.20156265>
- Rocchini, A. P., Moorehead, C., Wentz, E., & Deremer, S. (1987). Obesity-induced hypertension in the dog. *Hypertension (Dallas, Tex.: 1979)*, 9(6 Pt 2), III64-68. [https://doi.org/10.1161/01.hyp.9.6\\_pt\\_2.iii64](https://doi.org/10.1161/01.hyp.9.6_pt_2.iii64)
- Savic, R. M., & Karlsson, M. O. (2009). Importance of shrinkage in empirical bayes estimates for diagnostics: Problems and solutions. *The AAPS Journal*, 11(3), 558–569. <https://doi.org/10.1208/s12248-009-9133-0>
- Schinkel, A. H., Smit, J. J., van Tellingén, O., Beijnen, J. H., Wagenaar, E., van Deemter, L., Mol, C. A., van der Valk, M. A., Robanus-Maandag, E. C., & te Riele, H. P. (1994). Disruption of the mouse *mdr1a* P-glycoprotein gene leads to a deficiency in the blood-brain barrier and to increased sensitivity to drugs. *Cell*, 77(4), 491–502. [https://doi.org/10.1016/0092-8674\(94\)90212-7](https://doi.org/10.1016/0092-8674(94)90212-7)
- Solomon, s. (2020, January 5). *FDA Letter to Stakeholders: Do Not Use Ivermectin Intended for Animals as Treatment for COVID-19 in Humans*. FDA. <https://www.fda.gov/animal-veterinary/product-safety-information/fda-letter-stakeholders-do-not-use-ivermectin-intended-animals-treatment-covid-19-humans>
- Sutra, J. F., Chartier, C., Galtier, P., & Alvinerie, M. (1998). Determination of eprinomectin in plasma by high-performance liquid chromatography with

- automated solid phase extraction and fluorescence detection. *The Analyst*, 123(7), 1525–1527. <https://doi.org/10.1039/a802093k>
- Toutain, P. L., & Bousquet-Melou, A. (2004). Volumes of distribution. *Journal of Veterinary Pharmacology and Therapeutics*, 27(6), 441–453. <https://doi.org/10.1111/j.1365-2885.2004.00602.x>
- Verwaerde, P., Sénard, J. M., Galinier, M., Rougé, P., Massabuau, P., Galitzky, J., Berlan, M., Lafontan, M., & Montastruc, J. L. (1999). Changes in short-term variability of blood pressure and heart rate during the development of obesity-associated hypertension in high-fat fed dogs. *Journal of Hypertension*, 17(8), 1135–1143. <https://doi.org/10.1097/00004872-199917080-00013>
- Vora, A., Arora, V. K., Behera, D., & Tripathy, S. K. (2020). White paper on Ivermectin as a potential therapy for COVID-19. *Indian Journal of Tuberculosis*, 67(3), 448–451. <https://doi.org/10.1016/j.ijtb.2020.07.031>
- Wadman, M. (2020a). Why COVID-19 is more deadly in people with obesity—Even if they're young. *Science*. <https://doi.org/10.1126/science.abe7010>
- Wadman, M. (2020b). Why obesity worsens COVID-19. *Science*, 369(6509), 1280–1281. <https://doi.org/10.1126/science.369.6509.1280>
- Williamson, E. J., Walker, A. J., Bhaskaran, K., Bacon, S., Bates, C., Morton, C. E., Curtis, H. J., Mehrkar, A., Evans, D., Inglesby, P., Cockburn, J., McDonald, H. I., MacKenna, B., Tomlinson, L., Douglas, I. J., Rentsch, C. T., Mathur, R., Wong, A. Y. S., Grieve, R., ... Goldacre, B. (2020). Factors associated with COVID-19-related death using OpenSAFELY. *Nature*, 584(7821), 430–436. <https://doi.org/10.1038/s41586-020-2521-4>

